Proceedings

Enhanced, Compact and Ultra-Compact Heat Exchangers: Science, Engineering and Technology

Engineering Conferences International *Year* 2005

Keynote Lecture: Aspects of Two-Phase Flow Distribution at Header-Channels Assembly

S. Y. Lee J. K. Lee

Proceedings of Fifth International Conference on **Enhanced, Compact and Ultra-Compact Heat Exchangers: Science, Engineering and Technology**, Eds. R.K. Shah, M. Ishizuka, T.M. Rudy, and V.V. Wadekar, Engineering Conferences International, Hoboken, NJ, USA, September 2005.

CHE2005 – 46

ASPECTS OF TWO-PHASE FLOW DISTRIBUTION AT HEADER-CHANNELS ASSEMBLY

Sang Yong Lee[1] and Jun Kyoung Lee[2]

Department of Mechanical Engineering, Korea Advanced Institute of Science and Technology,
Science Town, Daejeon 305-701, Korea
E-mail: [1]sangyonglee@kaist.ac.kr, [2]JunKyoungLee@kaist.ac.kr

ABSTRACT

Flow distribution pattern of two-phase mixture from a header to parallel channels is examined extensively. The first part of this paper introduces the flow configuration at single T-junctions that can be considered as the unit elements of the header-channels assembly of the compact heat exchangers. Experimental observations and appropriate models for prediction of flow split to the branch are reported. Then the effect of the flow interaction between two neighboring channels (branches) on the flow split pattern is considered. Finally, to simulate practical shape of the header-channels assembly of compact heat exchangers, test sections with multiple parallel channels and a partitioned header were tested. Dependence of the flow distribution pattern on various operating conditions and header-channels configurations is presented. As a way to achieve an even distribution of the flow from the header to parallel channels, depth of the channel intrusion to the header wall was adjusted; and 1/8 of the header hydraulic diameter was found to be the optimum value of the intrusion depth.

INTRODUCTION

Problem of flow distribution from a partitioned header to parallel channels, as shown in Fig. 1, is becoming of interest in predicting heat transfer performance of compact heat exchangers. In many cases, due to the flow mal-distribution, the flow rates in the channels are not the same (Kim et al. (2003)). For two-phase flows, the situation becomes even worse because the phase separation effect becomes prominent due to large differences in density and viscosity between the gas and the liquid. In this paper, various aspects of two-phase flow distribution at the header-channels assembly are examined based on a series of experimental and modeling works performed up to date.

The first part of this paper introduces the flow configuration at single, dividing T-junctions that can be considered as unit elements of the header-channels assembly of the compact heat exchangers. In other words, the header-channels assembly is simulated as an accumulation of single T-junctions with their branches having a rectangular shape. Experimental observations and appropriate models for prediction of flow split to the branch are reported. Then the effect of the flow interaction between two neighboring channels on the flow split to the branches will be followed. Based on the single T-junction results, the effects of various operating

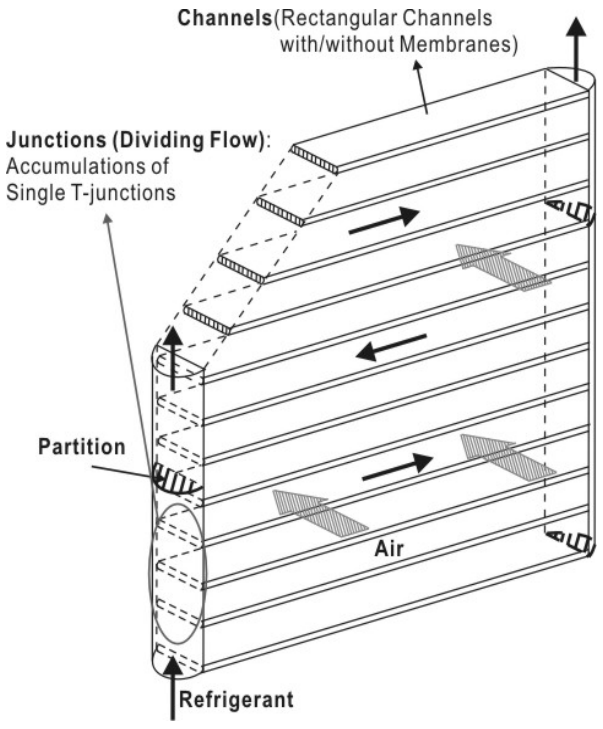

Fig. 1 Compact Heat Exchanger

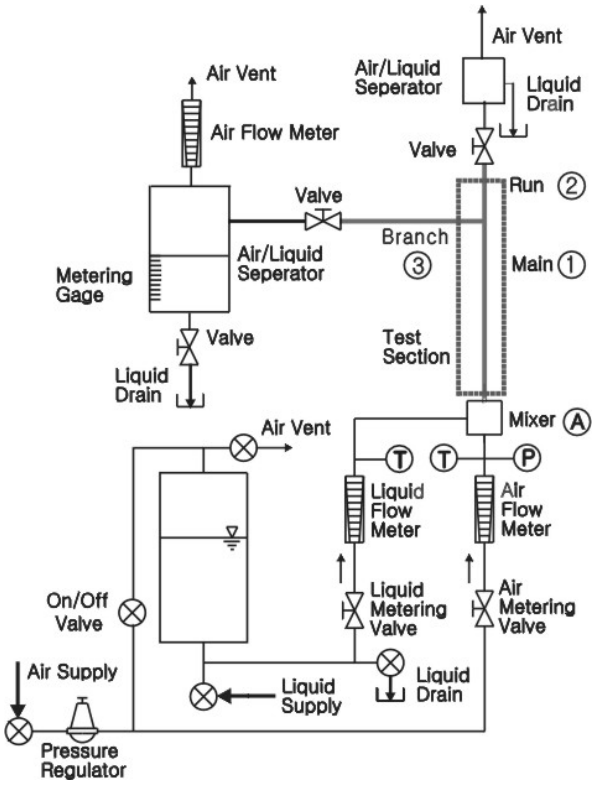

(a) Test Loop

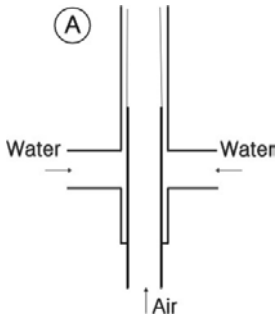

(b) Mixer

Fig. 2 Experimental Setup
(Lee and Lee (2001))

conditions and geometrical configurations for header-channels assemblies are presented, and possibility of achieving an even distribution from the header to parallel channels is going to be discussed.

TWO-PHASE FLOW AT SINGLE T-JUNCTIONS

Experimental Observations

Most of the previous works on the two-phase flow at dividing T-junctions were for larger than 30 mm in hydraulic diameter. (Azzopardi (1999), Reimann et al. (1988)) On the other hand, the hydraulic diameter of the headers of compact heat exchangers ranges mainly from 5 mm to 10 mm, and currently there are only a limited number of experimental studies available for this size range, represented by Hong (1978), Stacey et al. (2000) and Lee and Lee (2001). Figure 2(a) illustrates the experimental setup by Lee and Lee (2001), typical of this type of experiments. Water and air enter the mixer that consists of concentric tubes (Fig. 2(b)); air passes through the inner tube while water enters through the annulus. Thus an annular flow is formed at the entrance of the test section.

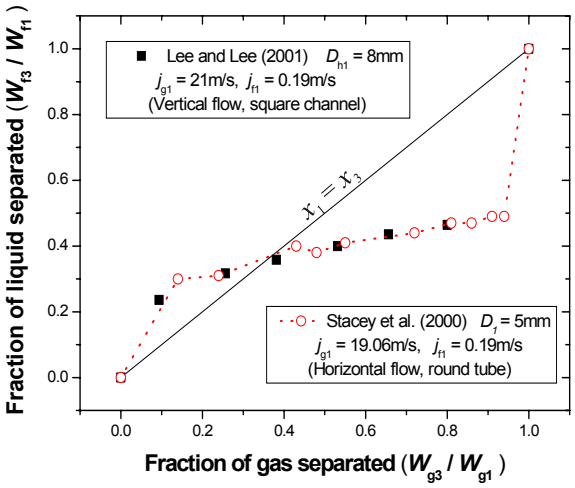

Fig. 3 Effects of Flow Direction and Cross-Sectional Shape of Main Channel
(Lee and Lee (2001))

Figure 3 shows a typical relationship between W_{f3}/W_{f1} and W_{g3}/W_{g1}, that are the fractions of liquid and gas splits to the branch, for a vertical flow in a square channel (Lee and Lee (2001)) and for a horizontal flow in a round tube (Stacey et al. (2000)). Under these flow conditions, the flow pattern in the main tube is considered annular. The straight diagonal line in the figure represents the cases of the same mass qualities in the main and in the branch, i.e., x_1=x_3; the data points at the lower left corner are the cases with very small flow rate to the branch while those at the upper right corner indicate high flow rates to the branch. The dividing annular flow generally exhibits an S-shape curve as shown in the figure depending on the momentum of the liquid film and the entrainment rate within the main channel. With the lower momentum of the liquid film, the fraction of the liquid split to the branch appears larger. On the other hand, with the higher liquid entrainment, the fraction of the liquid split decreases because the entrained drops tend to pass through the run along the gas stream. As seen in Fig. 3, little difference is found between the two cases even though the channel shapes and the orientations are different. This is because, in small T-junctions, the liquid film thickness along the periphery of the main channel is

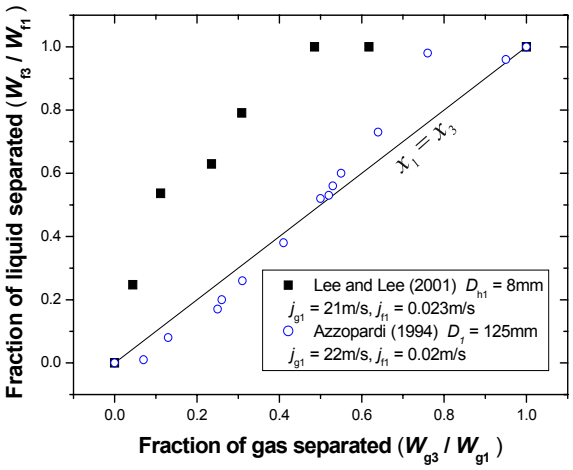

Fig. 4 Effect of T-junction Size
(Lee and Lee (2001))

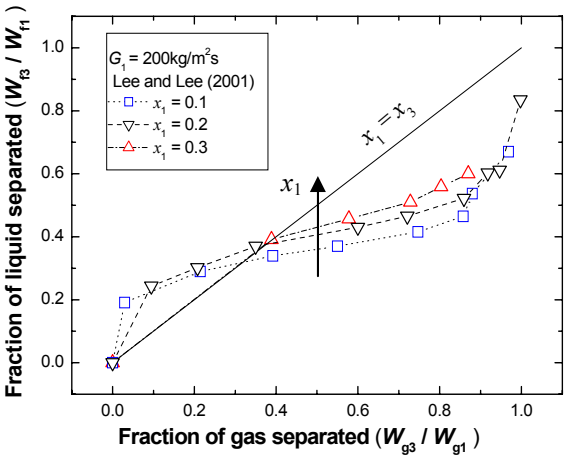

Fig. 6 Effect of Inlet Quality (x_1)
(Lee and Lee (2001))

almost the same, regardless of the channel shape and orientation as far as the gas and liquid momentum fluxes (or superficial velocities) remain unchanged. Asymmetry of the film thickness caused by the gravity force has been checked based on the result of Hurlburt and Newell (2000). They quantified the asymmetry of the liquid film thickness by using the ratio of the mean value to the thickness at the bottom of the horizontal pipe. For horizontal T-junctions (Stacey et al. (2000) and Hong (1978)), this ratio turned out to be within 0.7 – 0.9, which indicates a small asymmetry.

Figure 4 compares the fractions of the liquid and gas flow splits to the branch for a large T-junction (D_1 = 125 mm, Azzopardi (1994)) with those for the small T-junction case (D_{h1} = 8 mm, Lee and Lee (2001)). More amount of the liquid is split to the branch with the smaller T-junction; this is because the liquid film Reynolds number stays below the critical value for liquid entrainment, and less amount of the entrained liquid flows through the run along with the gas stream. Therefore, the large T-junction data are not applicable to the cases with small T-junctions.

Effect of the branch aspect ratio (or branch height, B_h) for a fixed width (or branch size) has been investigated by Lee and Lee (2001), as shown in Fig. 5. As the aspect ratio decreases, the fraction of the liquid split also decreases, but only slightly. Azzopardi (1984) has reported the similar trend for vertical large junctions (D_1 = 32 mm) with various aspect ratios of the branch (0.2 – 1.0) as well. This can be explained as follows: With the smaller aspect ratio (or size), the smaller region of the liquid film in the main channel is influenced by existence of the branch, but at the same time, the suction force to the branch also increases; and due to these competing effects, the rate of the liquid split decreases slightly with the branch aspect ratio.

Figure 6 shows the increasing trend of the fraction of the liquid split to the branch with the inlet quality at the main (x_1). This trend is the same with that of Collier (1976) (x_1 = 0.17 – 0.5). The gas momentum increases while the liquid momentum decreases with the larger inlet quality, and the liquid stream is more likely to be split to the branch.

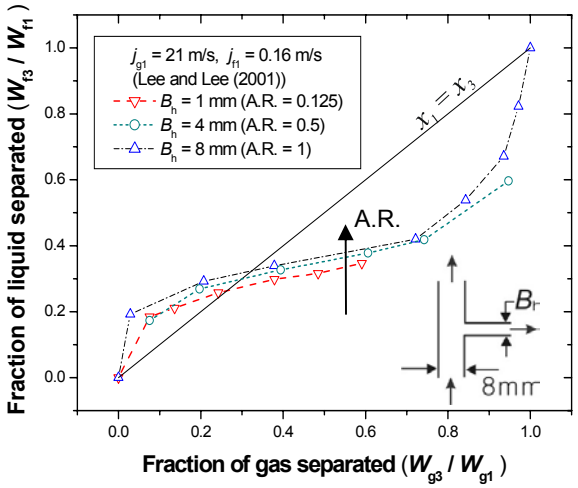

Fig. 5 Effect of Branch Aspect Ratio
(Lee and Lee (2001))

Flow Distribution Models

Several models have been developed for prediction of dividing T-junction flows (Azzopardi and Whalley (1982), Shoham et al. (1987), Hwang et al. (1988)), but those are basically for large-size T-junctions (D > 30 mm), which have never been tested for smaller sizes. Lee and Lee (2004b) have checked the applicability of those models to two-phase annular flow at small, dividing T-junctions (less than 10 mm in hydraulic diameter) using the experimental data by Hong (1978), Stacey et al.

Table 1
Prediction models for annular flow distribution at T-junction

Authors	Geometry, mm	Orientation *	Fluid	Remarks
Azzopardi and Whalley (1982)	$D_1 = D_2 = 32$ $D_3 = 6.35, 12.7, 19$	V	air-water	$a_f = a_g$
Shoham et al. (1987)	$D_1 = D_2 = D_3 = 51$	H	air-water	$a_f = a_g - \Delta r$
Hwang et al. (1988)	$D_1 = D_2 = D_3 = 38$	H	air-water	$R_g / R_f = \rho_g U_g^{\,2} / \rho_f U_f^{\,2} = (a_f / D_1)^{n_f} / (a_g / D_1)^{n_g}$

* : H and V denote horizontal and vertical flows, respectively.

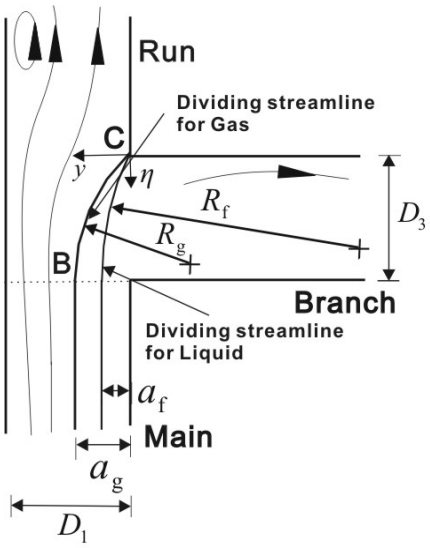

(a) Flow Configuration

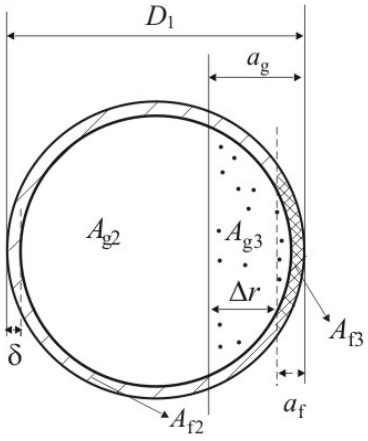

(b) Cross Section of Main Tube

Fig. 7. Illustration of Flow Model by Hwang et al. (1988)

(2000) and Lee and Lee (2001). Table 1 summarizes the prediction models tested.

Figure 7 illustrates the flow configuration considered based on the model by Hwang et al. (1988). In this figure, the dividing streamlines of the liquid and the gas flows are shown with their radii of curvature being R_f and R_g, respectively. Previously, Azzopardi and Whalley (1982) introduced the concept of "zone of influence" and assumed the boundary lines of the liquid and gas flows are the same, i.e., $a_f = a_g$. Here, when a part of the gas flow is split to the branch, the zone of influence is formed, and accordingly, a portion of the liquid flow belongs to that zone is also extracted from the main tube. The liquid flow through the branch is mainly from the film portion in the main tube rather than from the entrained drop-flow in the core portion because the liquid film has a lower velocity (momentum) than the liquid drops. Therefore, the proportion of the liquid film entering the branch was considered dependent simply on the gas flow rate flowing into the branch. Later, Azzopardi (1984) modified this model to take account of the effect of the diameter ratio between the branch and the main tube.

Based on the similar physical concept, Shoham et al. (1987) introduced a flow-pattern-dependent model to extend the applicable range to the larger dividing ratio, W_3/W_1. The model considers the inertial, centrifugal and damping forces on the liquid film having a boundary line, a_f, with no liquid entrainment to the gas stream, and the dividing gas streamline has an arc shape with the radius of curvature R_g. This model has an advantage of discriminating the liquid boundary line from the gas boundary line, and an appropriate correlation for Δr (= $a_g - a_f$) was proposed. In order to estimate the dividing ratio, the liquid film thickness should be given somehow, and Shoham et al. (1987) adopted the model by Taitel and Duckler (1976) to get this. The model works well for large T-junctions, as tested by Azzopardi (1994).

Hwang et al. (1988) proposed a physical model similar to that of Shoham et al. (1987), but with a different approach in obtaining the dividing streamlines

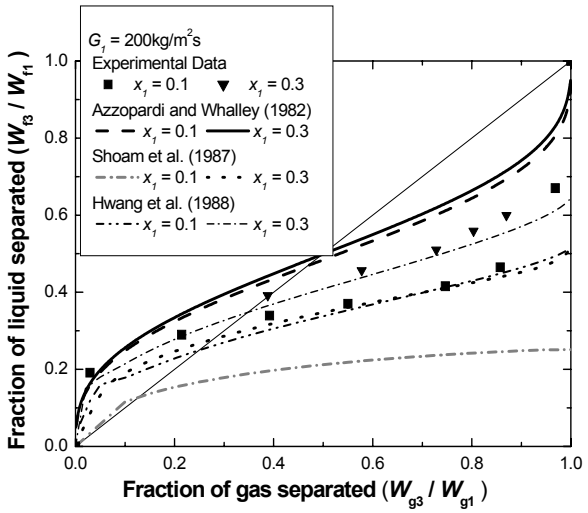

Fig. 8 Comparison between Experimental Results and Prediction Models: Effect of inlet quality (x_1) (Data by Lee and Lee (2001)) (Lee and Lee (2004b))

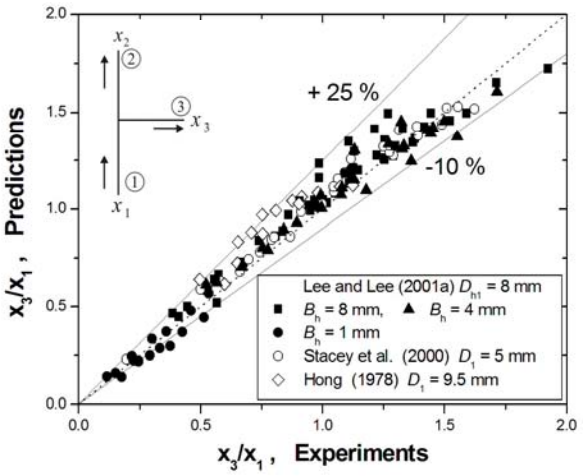

Fig. 9 Overall Evaluation of Prediction Model by Hwang et al.(1988) (Lee and Lee (2004b))

for the gas and the liquid flows, as illustrated in Fig. 7. For an annular flow, the acclerational and interfacial drag forces were considered negligible, and only the centrifugal force was considered important. Finally, they derived a relationship between the R_g/R_f as:

$$\frac{R_g}{R_f} = \frac{\rho_g U_g^{\ 2}}{\rho_f U_f^{\ 2}} = \left(\frac{a_f}{D_l}\right)^{n_f} \Bigg/ \left(\frac{a_g}{D_l}\right)^{n_g} \qquad (1)$$

where

$$n_k = 5 + 20\exp\{-53(a_k / D_l)\} \qquad (2)$$
(k = g (gas) or f (liquid))

Again, for this model, the film thickness and entrainment rate should be determined to predict the fraction of the flow split to the branch. Lee and Lee (2004b) adopted the approach of Whalley (1988), where the interfacial friction factor (or roughness correlation, Ambrosini et al. (1991)), triangular relationship (Asali et al. (1985)), and entrainment correlation (Hewitt and Govan (1990)) are considered.

Figure 8 shows the variation of W_{f3}/W_{f1} with W_{g3}/W_{g1} using the models of Azzopardi and Whalley (1982), Shoham et al. (1987) and Hwang et al. (1988) along with the experimental data by Lee and Lee (2001). Among them, the model of Hwang et al. (1988) was concluded the best in predicting the dividing flow behavior of two-phase mixtures. The overall accuracy in predicting the flow quality inside the branch is also high as shown in Fig. 9. This is because the streamline shapes are better represented by the Hwang et al.'s model in describing the dividing flow configuration at the junction.

Effect of Channel Spacing

For most of the compact heat exchangers, distance between the parallel channels (S) is comparable to or even smaller than the hydraulic diameter of the header. Thus the flow interaction between the junctions should be taken into account carefully. This effect becomes more prominent if the distance between the channels gets closer. Figure 10 illustrates the test section consists of two horizontal parallel channels and a header used by Lee and Lee (2003) to check the channel (branch) spacing

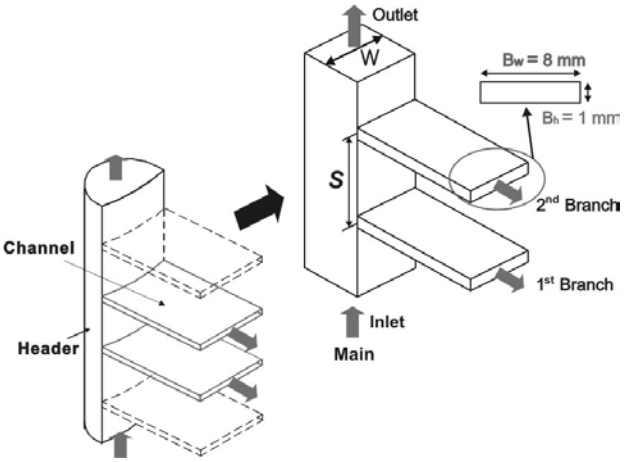

Fig. 10 Channel Array of Compact Heat Exchanger

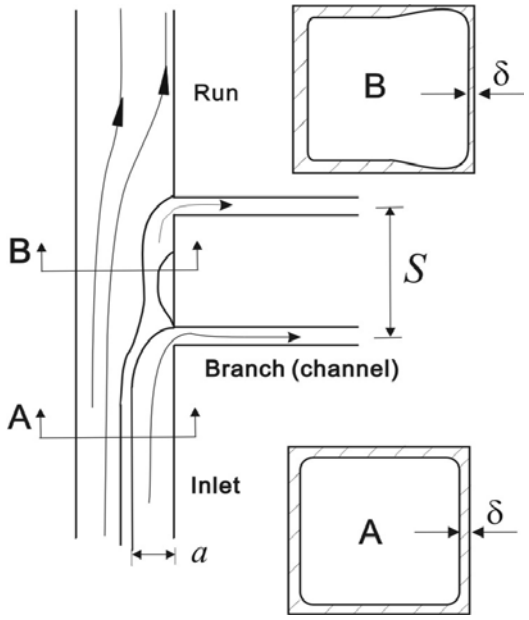

Fig. 11 Schematic Flow Configuration

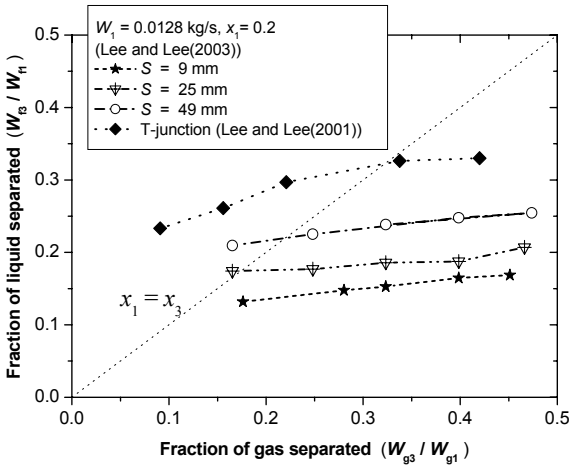

Fig. 12 Effect of Distance between Channels (*S*) (Lee and Lee (2003))

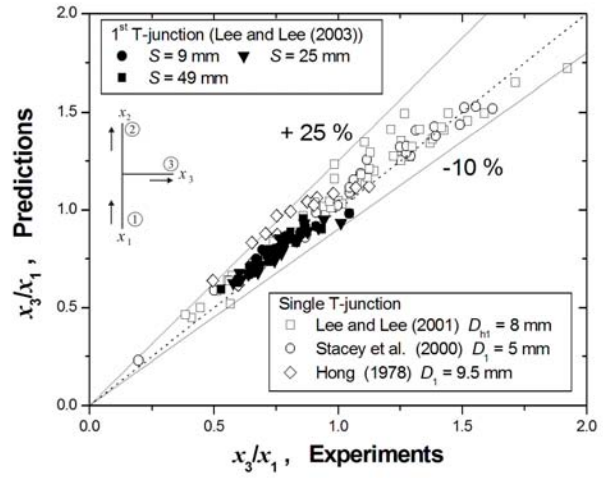

(a) Upstream Channel

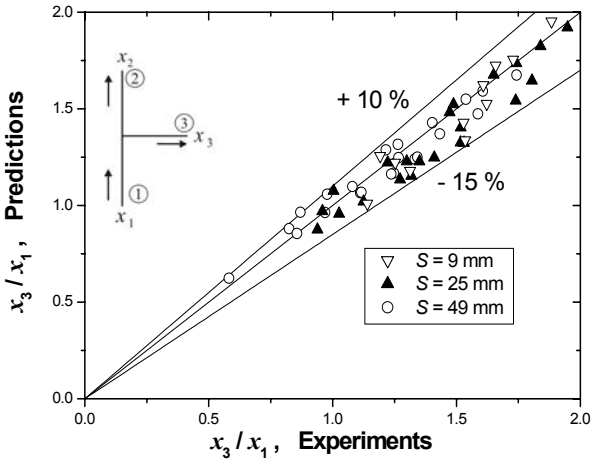

(b) Downstream Channel

Fig. 13 Prediction of Flow Distribution (Lee and Lee (2003))

effect on the flow split. In their work, the second T-junction was chosen as the reference junction because the flow disturbance propagates mostly in the downstream direction and the backward flow disturbance (from the second junction to the first one) was considered insignificant.

According to Lee and Lee (2003), the liquid flow rate is always smaller at the second branch than at the first branch, while the gas flow rates in those two branches remain approximately the same. As illustrated in Fig. 11, it is easy for the liquid annulus to be separated out to upon arrival at the entrance of the first branch, and the rest amount of the liquid film flows through the subsequent branch. With the smaller branch spacing, the liquid film reaches the next branch without being redistributed to have a uniform thickness, and the amount of the liquid split to the second branch decreases. Figure 12 shows the effect of the branch spacing (*S*) on the flow distribution to each branch. The fraction of the liquid split to the second branch decreases with the smaller branch spacing, and far more deviates from the single T-junction case reported by Lee and Lee (2001). In other words, with a large branch spacing, amount of the flow split can be predicted using the single T-junction model without any serious error, as easily imagined.

The effect of the channel spacing can be taken into account in predicting the flow split to the parallel branches by modifying Eq. (2) originally proposed by Hwang et al. (1988) as:

$$n_k = C\left[5 + 20\exp\left\{-53(a_k / D_1)\right\}\right] \qquad (3)$$

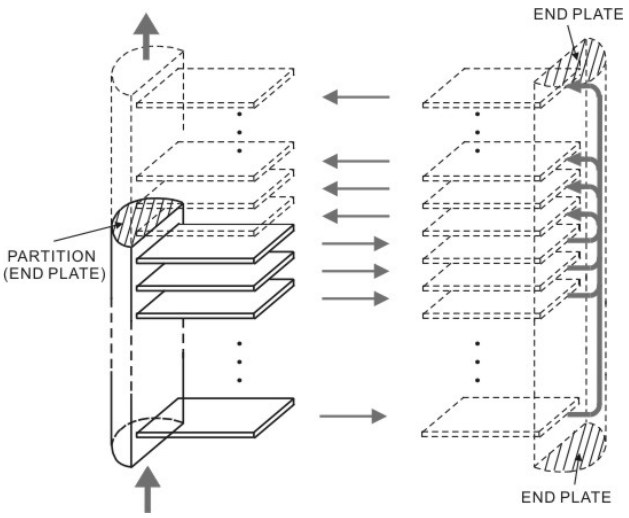

Fig. 14 Illustration of Header-Channels Flow in a 2-pass Heat Exchanger

with

$$C = 1 \qquad \text{(Upstream T-junction)} \qquad (4)$$

$$C = \left(1 + 47\frac{B_h}{S}\right)^{-0.43} \qquad \text{(Downstream T-junction)} \qquad (5)$$

where C considers the upstream junction effect (Lee (2005b)). Equations (3) - (5) well represent the measured results for the upstream (Fig. 13(a)) and the downstream junctions (Fig. 13(b)). It should be mentioned that these equations represent the channel spacing effect better than the correlation proposed by Lee and Lee (2003, 2004c) that is based on the model by Shoham et al. (1987).

TWO-PHASE FLOW DISTRIBUTION FROM A HEADER TO MULTIPLE PARALLEL CHANNELS

General Flow behavior

This time we extend our discussions on the flow distribution of two-phase mixture from a partitioned header to multiple parallel channels that are much closer to the practical shape of compact heat exchangers as illustrated in Fig. 14.

Lee and Lee (2004c) have used a test loop shown in Fig. 15 that is basically the same with the experimental setup in Fig. 2, except for the test section. The two-phase mixture flows upwards through a square vertical header connected to fifteen (15) parallel, horizontal rectangular channels. An end plate (partition) was installed at the most downstream of the header. The experiments were carried out for the annular flow regime at the header inlet

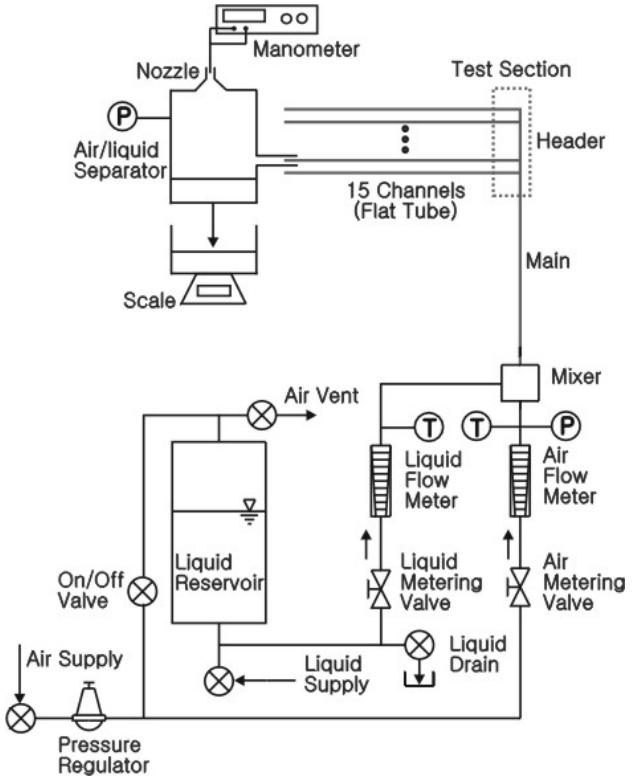

(a) Test Loop

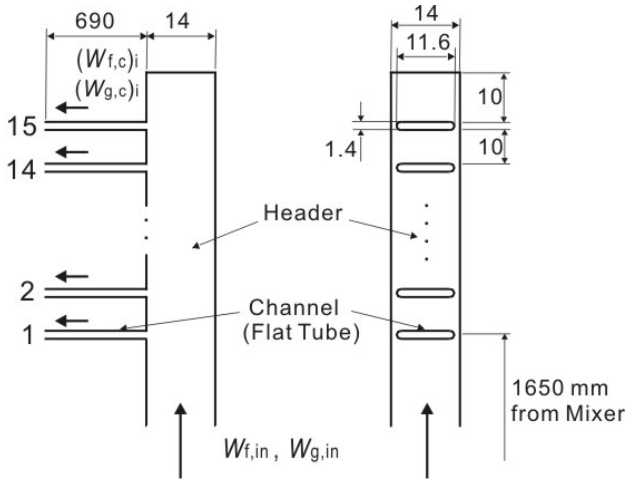

(b) Configuration of Test Section

Fig. 15 Experimental Setup for Multiple-channel Experiments (Lee and Lee (2004c))

because this flow pattern is mostly probable to occur once the mass quality becomes large, say larger than 0.1.

Figure 16 shows a typical distribution shape along with a flow-visualized result. In Fig. 16(a), the abscissa represents the channel number counted from the header inlet while the ordinate the flow rates of the liquid (water)

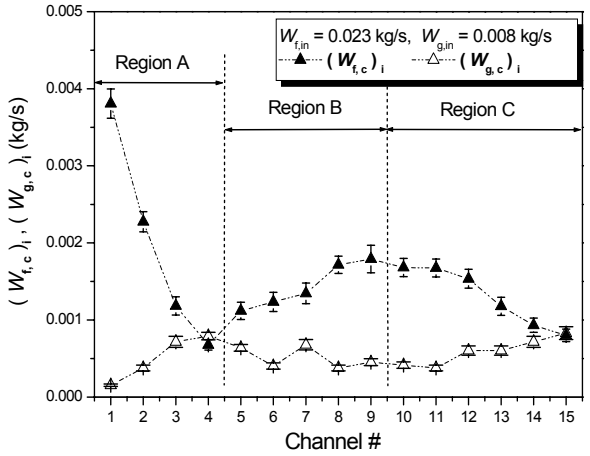

(a) Flow Distributions

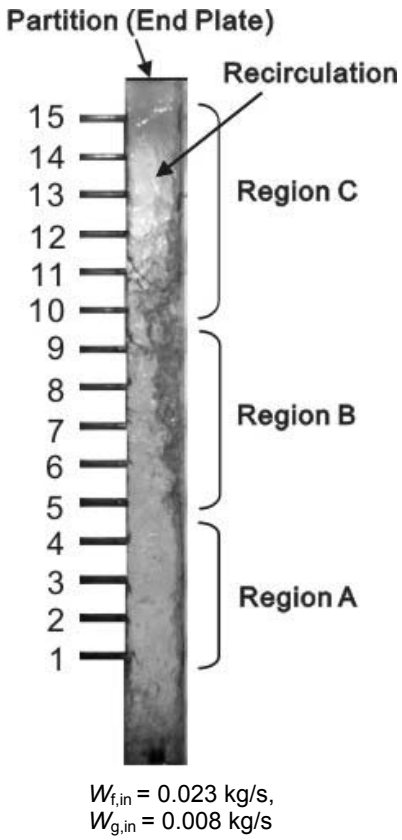

(b) Flow Visualization

Fig. 16 Effect of End Plate on Flow Configuration inside Header (Lee and Lee (2004c))

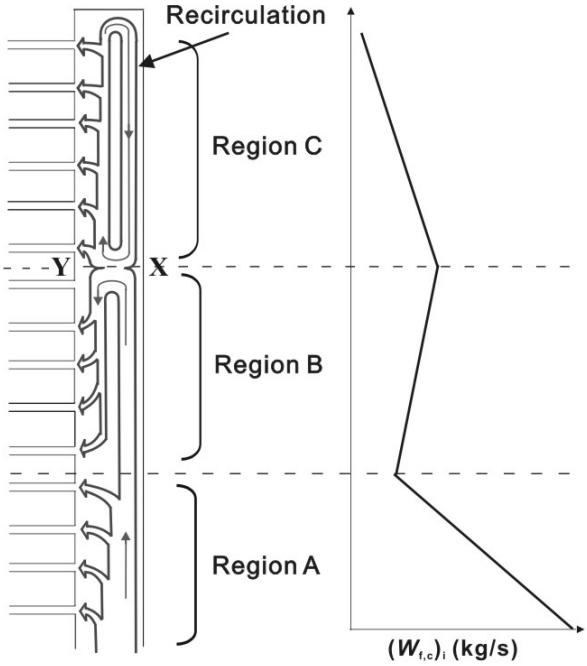

Fig. 17 Schematic Flow Configuration and General Trend of the Liquid Flow Distribution (Lee and Lee (2004c))

and the gas (air) separated out through each channel, denoted as $(W_{f,c})_i$ and $(W_{g,c})_i$, respectively. In general, at the fore part of the header (channels #1 - #4, region A), less amount of liquid flow is separated out through the channels as the two-phase mixture proceeds in the downstream direction. In the middle part of the header (channels #5 - #9, region B), the trend becomes reversed. On the other hand, near the end plate (channels #10 - #15, region C), the trend appears similar to that in region A. For the gas flow distribution, the trend is exactly opposite; increases, decreases and then increases again as flows along the header. This is because, to maintain the same pressure drops across the long parallel channels, the gas flow rate should be small in a channel where the liquid flow rate is large. However, the variation in the distribution shape of the gas flow appears minor compared to that of the liquid flow distribution.

To help understanding the flow distribution shape, the header part was visualized using a CCD camera as in Fig. 16(b), and the flow configuration is illustrated in Fig. 17. A large flow recirculation is found near the end plate of the header, which makes the flow structure much complicated. In region A, the downstream effect (the end-plate effect) did not appear at all. A portion of the liquid film flows out through the first channel upon arrival at the corresponding entrance, and the rest amount of the liquid flows through the subsequent channels with the smaller flow rates as proceeds downstream. On the other hand, in region C, a strong local recirculation occurs in the clockwise direction and the downstream effect predominates. Region B is the transition zone between regions A and C. A portion of the downward liquid flow in region C collides and mixes with the upward liquid flow at point X in the right hand side, and then cross the header to the stagnation point Y in the left

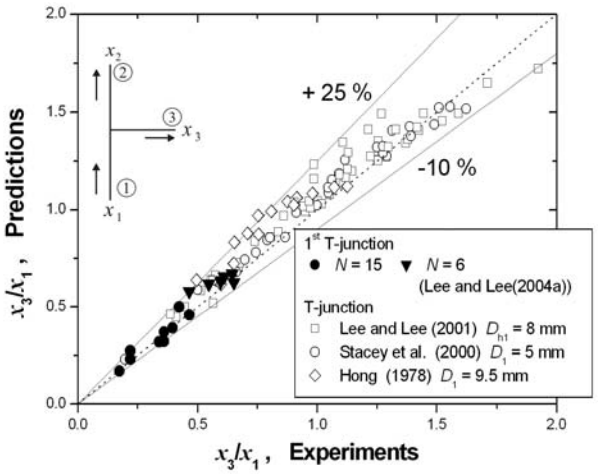

(a) 1st channel

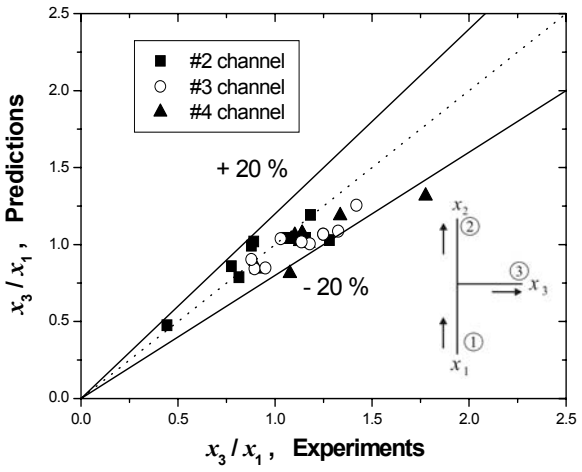

(b) #2 - #4 channels

Fig. 18 Prediction of Flow Distribution at Header-Channel Junctions (Lee and Lee (2004c))

hand side. (See Fig. 17.) Thereafter the flow is divided into upward and downward streams to be separated out to the parallel channels in regions C and B, respectively. Though the liquid distributions in regions A and C have the same trend, the variation in region C is smaller compared to that in region A. This is because, due to a strong mixing effect by the flow recirculation, the flow distributions through the channels tend to be even in region C.

Since the downstream effect does not appear in region A (channels #1-#4), the branching flow rate in this region can be reasonably predicted using Eqs. (3) – (5), and the results are shown in Fig. 18. However, for other regions (i.e., B and C), no appropriate prediction model has been reported for the flow distribution; probably the homogeneous two-phase flow model may be applicable because of the strong mixing effect by the flow recirculation.

Geometrical Shape Effects

In this section, the effect of the geometrical shape of the header-channels assembly is going to be discussed; namely, the effects of the membranes in channels, the channel spacing and the intrusion depth.

Figure 19 shows the cross sections of the extruded aluminum tube with six sub-channels (Lee (2005b)). In the same figure, a plain rectangular channel is also shown for comparison purpose. The total flow area of the channel with the membranes is 16.3 mm^2 that is almost the same with the flow area of the plain channel, 16.2 mm^2. Here, a test section with 15 parallel channels similar to that in Fig. 15(b) was used. The measured results on the liquid and the gas flow distributions, as shown in Fig. 20, are not much different from those without the membranes. The only notable thing is that, especially for the gas distribution, the flow rate difference between the neighboring channels appears smaller and the distribution pattern tends to be rather even. This implies that the two-phase flow configuration inside the header (as shown in Fig. 16) plays the major role in determining the flow distribution.

In the earlier part of this paper, the effect of the channel (branch) spacing for a test section with two parallel branches (Fig.10) was discussed. Lee and Lee (2005a) have repeated the effect of the channel spacing using a test section with six parallel channels and an end plate, simulating the header-channels junction of the compact heat exchangers. At the same time, the effect of the intrusion depth of the channel entrances to the header wall on the flow distribution was tested. Figure 21 shows the configuration of the test section, where S and H denote the channel spacing and the intrusion depth to the header wall.

Figure 22 shows a typical distribution pattern of the liquid and gas flows to the channels for different channel distances (S), but with zero intrusion depth, H = 0. Basically the distribution pattens are the same with that shown in Fig. 16, obtained by Lee and Lee (2004c) for the test section with 15 channels. The only different thing is the relative size of each region. With the larger channel spacing, region C becomes relatively smaller (compared to the size of the entire region) while region A remains unchanged. Thus region B appears to be relatively larger. Figure 23 shows a flow visualization result and an illustration of the channel spacing effect on the header flow configuration. In Fig. 22, the previous results by Lee and Lee (2004a) were plotted together for comparison. Again, the trend is the same even though the sizes of the header and the channel cross-sections are different. It should be mentioned that the header cross-section size appears less influential than the channel spacing. The gas flow distribution is almost insensitive to the channel spacing and the header size.

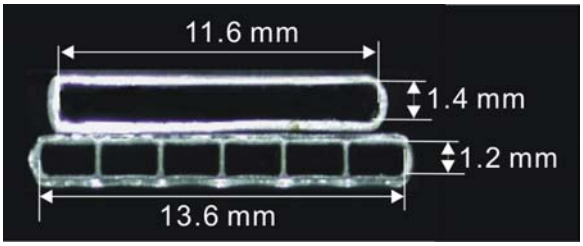

Fig. 19 Cross Sections of the Channels with and without Membranes (Lee and Lee (2005b))

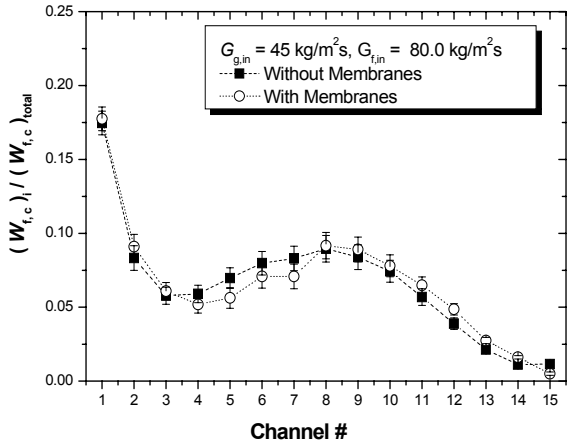

(a) Liquid distribution

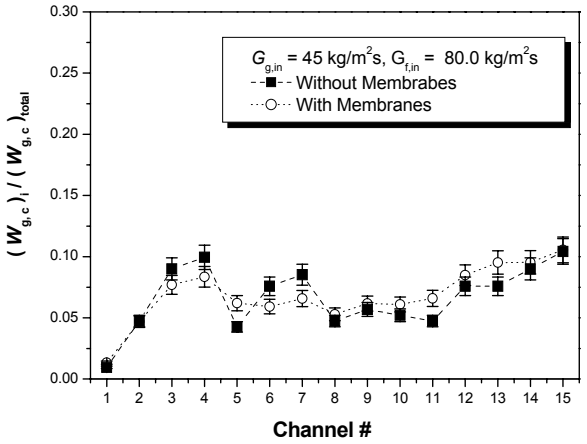

(b) Gas distribution

Fig.20 Effect of Membranes in Channels (Lee and Lee (2005b))

Figure 24 is a typical result showing the effect of the intrusion depth. The dashed horizontal lines in the figure represent the case with even distributions of the liquid and the gas flows. With the zero intrusion depth (H = 0 mm), more amount of liquid is split out to the channels at the fore part of the header. On the other hand, the trend becomes reversed with a deep intrusion depth (H = 7 mm). The same trend has been reported by Lee and Lee (2004a). This is because the intruded part hinders the

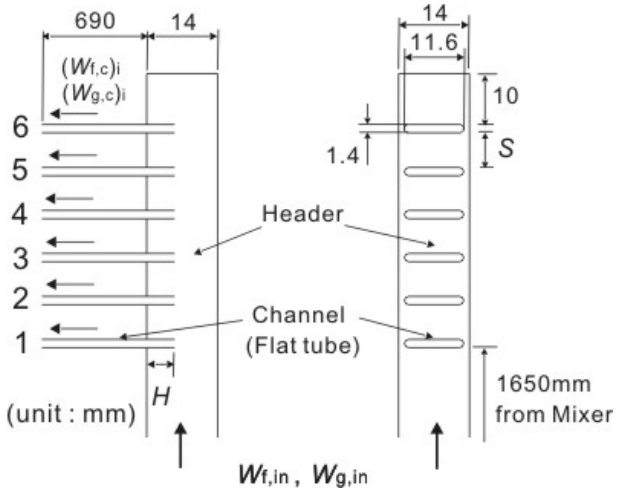

Fig. 21 Configuration of Test Section for Six-Channel Experiments (Lee and Lee (2005a))

liquid flow (liquid film) inside the header from being separated out through the channels (This can be confirmed through flow visualization as demonstrated in Fig. 25(a) for H/D_h = 1/2). This tells that there should be an optimum value of the intrusion depth for even flow distribution, staying between zero and 7 mm; and the test results give 1.75 mm as the optimum value, corresponding to 1/8 of the header hydraulic diameter. The same results were obtained for H/D_h = 1/8 with different channel spacing as shown in Fig. 26. The flow behavior with the optimum value of H/D_h is visualized in Fig. 25(b). The photographs show that the liquid and the gas flows inside the headers are well mixed with each other regardless of the distance between the channels. As a consequence, the liquid flow distribution to the channels tends to be even. The results of Lee and Lee (2004a) were also plotted to show the same value of the optimum intrusion depth, $D_h/8$. It is interesting to note that the ratio of the optimum intrusion depth to the header size (H/D_h) appears to be about the same, 1/8, for practical ranges of the flow rate (G_{in} = 70 - 165 kg/m^{2}s), mass quality (x_{in} = 0.3 – 0.7), channel distance (S = 10 – 21.5 mm) and the header size ($D_{h,in}$ = 14 – 24 mm). At the same time, the gas separation rate to the channels remains even as shown in Fig. 26.

CONCLUSION

In the present paper, various aspects of the flow distribution of two-phase mixture in small-scale header-channels assembly have been investigated. As a fundamental approach, two-phase dividing (branching) flow at single T-junctions has been studied with the effects of the flow rate (W_{in}) and quality of the mixture (x_{in}), channel size ($D_{h,in}$) and orientation, and distance

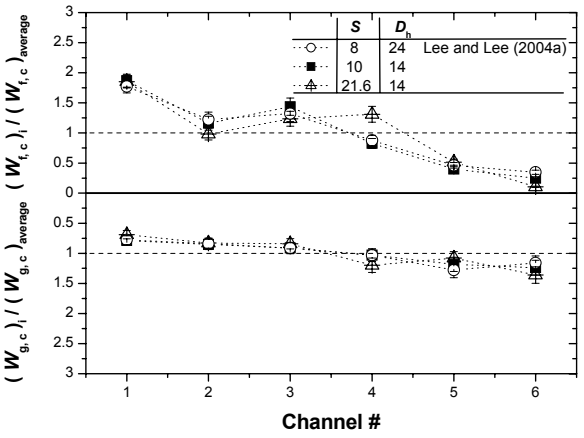

Fig. 22 Effect of Distance between Channels (S) (H = 0, G_{in} = 70 kg/m^{2}s, x_{in} = 0.45) (Lee and Lee (2005a))

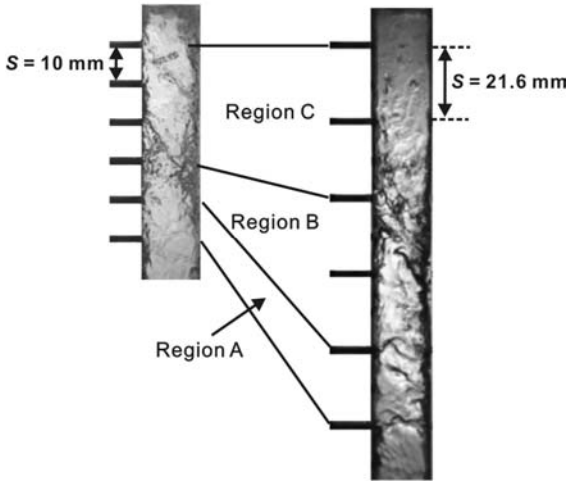

G_{in} = 70 kg/m^{2}s, x_{in} = 0.45

(a) Flow visualization

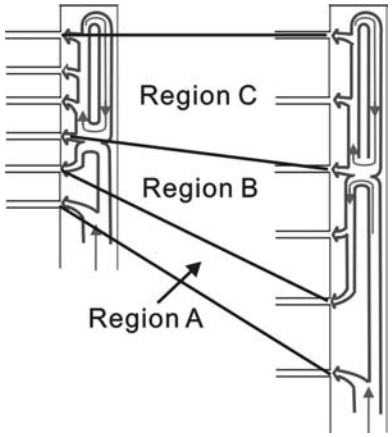

(b) Schematic flow configuration

Fig. 23 Effect of Distance between Channels (S) on Header Flow Configuration (Lee and Lee (2005a))

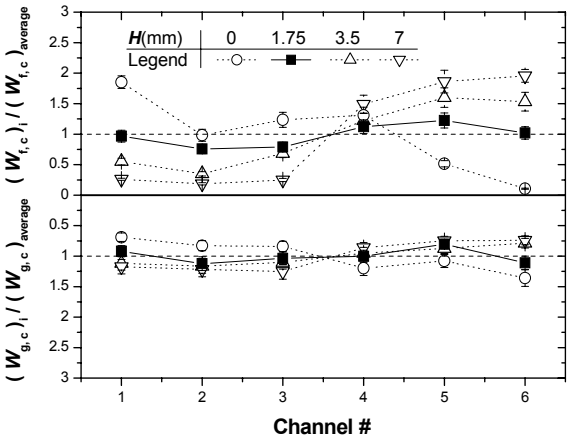

Fig. 24 Effect of Intrusion Depth (H) on Flow Distribution (D_h = 14 mm, S = 21.6 mm, G_{in} = 70 kg/m^{2}s, x_{in} = 0.45) (Lee and Lee (2005a))

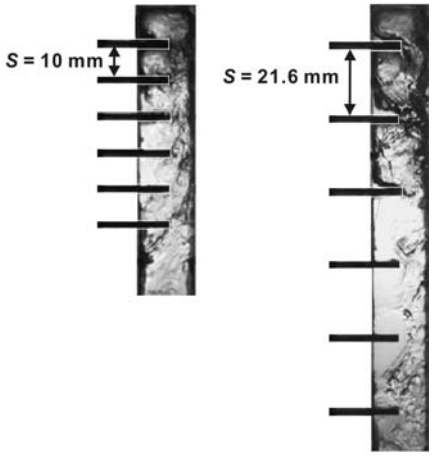

(a) H/D_h = 1/2

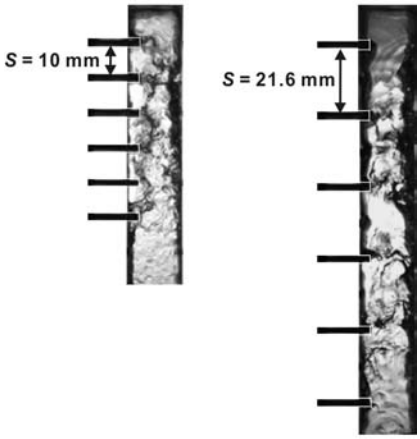

(b) H/D_h = 1/8

Fig. 25 Flow Visualization of Effect of Intrusion Depth (H) on Flow Configuration with Different Distance between Channels (D_h = 14 mm, G_{in} = 70 kg/m^{2}s, x_{in} = 0.45)

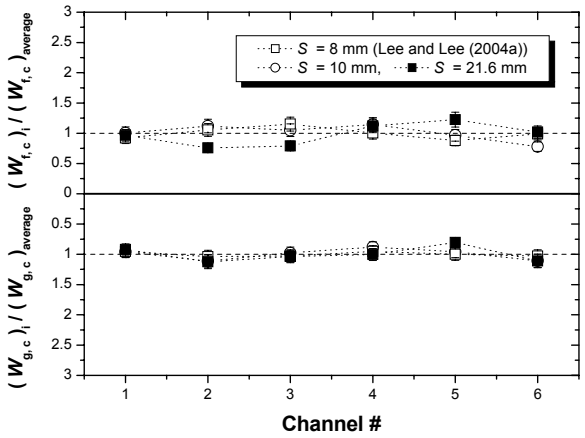

Fig. 26 Effect of Distance between Channels for Intrusion Depth of H/D_h = 1/8 (G_{in} = 70 kg/m^{2}s, x_{in} = 0.45) (Lee and Lee (2005a))

between the channels (S) taken into account. Prediction models, originally developed for large T-junctions, were assessed based on the experimental results. Among the prediction models tested, the model by Hwang et al. (1988) was concluded to be the most appropriate. Then, to simulate the practical shape of the header-channels assembly of compact heat exchangers, test sections with multiple parallel channels and a partitioned header were tested. The header flow consists of three regions, where the rate of the liquid flow split to the channels decreases, increases and then decreases along the downstream direction. The rate of the liquid flow split to the channels near the entrance of the header was well predicted by the modified model for single T-junctions since this region is not affected by existence of the end plate (partition). For the other regions, where the local flow recirculation effect predominates, no prediction model has been proposed up to date. The distribution pattern is relatively insensitive to existence of the membranes inside the channels or the spacing between the channels (S). On the other hand, the distribution pattern is strongly influenced by the two-phase flow configuration inside the header, which is easily controlled by adjusting the depth of the channel intrusion to the header wall (H). The optimum value of the intrusion depth for even distributions of the liquid and the gas flows to the channels was found to be about 1/8 of the header hydraulic diameter.

ACKNOWLEDGEMENT

This work was supported by the Ministry of Commerce, Industry and Energy, and in part by the Brain Korea 21 Project.

NOMENCLATURE

a	distance of streamline A-B (in Fig.7) from the pipe wall on the branch side [m]
B_h	branch height [m]
B_w	branch width [m]
C	empirical correction factor
D	diameter [m]
D_h	hydraulic diameter [m]
G	mass flux [kg/m^{2}s]
H	intrusion depth of the channel [m]
j	superficial velocity [m/s]
N	number of channels
n	exponent for streamline curvature correlation
R	radius of curvature [m]
S	distance between channels (branches) [m]
Δr	distance between boundary lines of gas and liquid flows, $a_g - a_f$ [m]
U	velocity [m/s]
W	mass flow rate [kg/s]
x	quality, $W_g/(W_g + W_f)$

Greek letters

δ	liquid film thickness [m]
ρ	density [kg/m^3]

Subscripts

1	main tube
2	run
3	branch
f	liquid
g	gas
i	index (channel numbers)
in	header (main tube) inlet

REFERENCES

Ambrosini, W., Andreussi, P. and Azzopardi, B. J., 1991, A physically based correlation for drop size in annular flow, *Int. J. Multiphase Flow*, Vol. 17, pp. 497-507.

Asali, J. C., Hanratty, T. J. and Andreussi, P., 1985, Interfacial drag and film height for vertical annular flow. *A.I.Ch.E. J.*, Vol. 31, pp. 895-902.

Azzopardi, B. J., 1984, The effect of side arm diameter on two phase flow split at a T junction, *Int. J Multiphase Flow*, Vol. 10, pp. 509-512.

Azzopardi, B. J., 1994, The split of vertical annular

flow at a large diameter T junction, *Int. J Multiphase Flow*, Vol. 20, pp. 1071-1083.

Azzopardi, B. J., 1999, Phase separation at T-junctions, *Multiphase Science and Technology*, Vol. 11, pp. 223 – 329.

Azzopardi, B. J. and Whalley, P. B., 1982, The effect of flow patterns on two phase flow in a T junction, *Int. J Multiphase Flow*, Vol. 8, pp. 491-507.

Collier, J. G., 1976, Single-phase and two-phase behavior in primary circuit components, *Proc. N.A.T.O. Advanced Study Institute on Two-phase Flow and Heat Transfer*, Istanbul, Turkey, Hemisphere, Washington, D.C., pp.322-333.

Hewitt, G. F. and Govan, A. H., 1990, Phenomenological modeling of non-equilibrium flows with phase change, *Int. J. Multiphase Flow*, Vol. 33, pp. 229-242.

Hong, K. C., 1978, Two phase flow splitting at a pipe tee, *J. Pet. Technol.*, pp.290-296.

Hurlburt, E. T. and Newell, T. A., 2000, Prediction of the circumferential film thickness distribution in horizontal annular gas-liquid flow, *J. Fluids Engineering*, Trans. ASME., Vol.122, pp. 396-402.

Hwang, S. T., Soliman, H. M. and Lahey, R. T., Jr, 1988, Phase separation in dividing two-phase flows, *Int. J. Multiphase Flow*, Vol.14, pp. 439-458.

Kim, M. H., Lee, S. Y., Mehendale, S. S. and Webb, R. L., 2003, Microchannel heat exchanger design for evaporator and condenser applications, *Advances in Heat Transfer*, Vol. 37, pp. 297-429.

Lee, J. K. and Lee, S. Y., 2001, Dividing two-phase annular flow within a small vertical rectangular channel with a horizontal branch, *Proc. 3rd International Conference on Compact Heat Exchangers and Enhancement Technology for the Process Industries*, Davos, Switzerland, pp.361-368.

Lee, J. K. and Lee, S. Y., 2003, Branching of two-phase flow from a vertical header to horizontal parallel channels, *Proc. 4th International Conference on Compact Heat Exchangers and Enhancement Technology for the Process Industries*, Crete Island, Greece, pp.309-316.

Lee, J. K. and Lee, S. Y., 2004a, Distribution of two-phase annular flow at header–channel junctions, *Experimental Thermal and Fluid Science,* Vol. 28, pp. 217-222.

Lee, J. K. and Lee, S. Y., 2004b, Assessment of models for dividing two-phase flow at small T-junctions, *Proc. 5th International Conference on Multiphase Flow*, Yokohama, Japan, Paper No. 565.

Lee, J. K. and Lee, S. Y., 2004c, Two-phase flow behavior inside a header connected to multiple parallel channels, *Proc. 3rd International Symposium on Two-phase Flow Modelling and Experimentation*, Pisa, Italy.

Lee, J. K. and Lee, S. Y., 2005a, Optimum channel intrusion depth for uniform flow distribution at header-channel junctions, *Proc. 6th KSME-JSME Thermal & Fluids Engineering Conference*, Jeju, Korea.

Lee, J. K. 2005b, An Experimental Study on Two-Phase Flow Distribution at Header-Channel Junctions of a Compact Heat Exchanger, Ph.D. Dissertation (in preparation), Department of Mechanical Engineering, KAIST.

Reimann, J., Brinkmann, H. J. and Domanski, R., 1988, gas-liquid flow in dividing T-juncton with horizontal inlet and different branch orientations and diameters, Kernforschungszentrum Karlsruhe, Institute fur Reaktorbauelemente Report KfK 4399, pp. 105 – 119.

Shoam, O., Brill, J. P. and Taitel, Y., 1987, Two-phase flow splitting in a tee junction - experimental and modelling, *Chem. Eng. Sci.*, Vol .42, pp. 2667-2676.

Stacey, T., Azzopardi, B. J. and Conte, G., 2000, The split of annular two phase flow at a small diameter T-junction, *Int. J Multiphase Flow*, Vol. 26, pp. 845-856.

Taitel, Y. and Dukler, A. E. 1976, A model for predicting flow regime transition in horizontal and near horizontal gas-liquid flow, *AIChE J.*, Vol. 24, pp. 920-934.

Whalley, P. B., 1988, Boiling, condensation and gas-liquid flow, *Oxford Science Publications*.